IEEE Access
Multidisciplinary | Rapid Review | Open Access Journal

Received 15 July 2024, accepted 6 August 2024, date of publication 9 August 2024, date of current version 30 August 2024.

Digital Object Identifier 10.1109/ACCESS.2024.3441316

RESEARCH ARTICLE

Millimeter Wave Wideband and Low-Loss Compact Power Divider Based on Gap Waveguide: For Use in Wideband Antenna Array System

AREFEH KALANTARI KHANDANI[1], ALI FARAHBAKHSH[1,2], DAVOOD ZARIFI[2,3], AND ASHRAF UZ ZAMAN[4], (Senior Member, IEEE)

[1]Department of Electrical and Computer Engineering, Graduate University of Advanced Technology, Kerman 7631133131, Iran
[2]Department of Microwave and Antenna Engineering, Faculty of Electronics, Telecommunications, and Informatics, Gdańsk University of Technology, 80-233 Gdańsk, Poland
[3]School of Electrical and Computer Engineering, University of Kashan, Kashan 87317-53153, Iran
[4]Department of Signals and Systems, Chalmers University of Technology, 412 96 Gothenburg, Sweden

Corresponding author: Ali Farahbakhsh (ali.farahbakhsh@pg.edu.pl)

ABSTRACT This paper presents a wideband and low-loss design of a compact power divider based on gap waveguide technology. The proposed power divider consists of two adjacent E-plane groove gap waveguide and a small ridge section to couple and equally divide the EM energy from the input E-plane groove gap waveguide to the two output ones in-phase. The simulation results show that the proposed waveguide power divider has about 40% impedance bandwidth while its size is $0.7\lambda \times 0.6\lambda$ at the center frequency. An 8-way power divider is designed using the proposed 2-way power divider and the back-to-back configuration of the 8-way one is fabricated to investigate the performance of the proposed design. In addition, to show the application of the presented power divider, a wideband linear horn antenna array is designed and fabricated. The measured results agree well with the simulated ones and prove the excellent low-loss and wide bandwidth of the proposed power divider over the band of interest from 50-75GHz. The measured S_{11} of the entire 8-way power divider remains below -10 dB level, the insertion loss is around 1 dB over the band of interest. Also, the S_{11} of the horn array integrated with the 8-way feed network remains below -10 dB and the low sidelobes of the radiation pattern of the entire horn array indicates excellent phase and amplitude balance for the power divider over the entire bandwidth of interest.

INDEX TERMS Compact power divider, E-plane groove gap waveguide, mmWave, ridge gap waveguide, wideband design.

I. INTRODUCTION

Power dividers are essential components for distributing or combining signals in wireless communication and radar systems and satellite links. They have various applications in couplers, diplexers and antenna array design, such as feeding networks, and beamforming networks [1], [2], [3], [4], [5]. Another application of power dividers is in high power amplifier (HPA) design where several power amplifiers need to operate in parallel fashion [6]. HPAs are used to amplify signals to high power levels for transmission purposes. However, HPAs are usually bulky, expensive and have complex geometries at mmWave frequencies [7], [8]. Power dividers can be used to split the input RF signal into several parallel paths and feed them to multiple power amplifiers (LPAs) to avoid saturation issue. The output signals from the LPAs can then be combined by another power divider to obtain a high output power. This way, power dividers can enable the use of smaller, cheaper and more efficient LPAs instead of a single HPA [9], [10]. Power dividers can also improve the linearity,

The associate editor coordinating the review of this manuscript and approving it for publication was Feng Wei.

bandwidth and reliability of the HPA system by reducing the nonlinear distortion and mismatch effects. At millimeter-wave (mmWave) frequencies, power dividers need to have low loss, high isolation and compact size to achieve high performance and efficiency [11], [12], [13], [14], [15], [16], [17]. Also, compact power dividers are needed in case of high efficiency planar slot array antennas where waveguide based corporate feeding networks are typically used [18], [19].

As the applications of mmWave power dividers increase, designing a compact power divider becomes more essential for reducing the volume, weight and manufacturing cost of the systems. Moreover, compactness is crucial for achieving wide bandwidth and low insertion loss and reducing the heat dissipation and thermal stress by minimizing the volume and surface area of the device [20], [21], [22], [23], [24].

Different types of power dividers can be designed using various technologies, which have been studied extensively in the literature. One type of technology is based on using substrates, such as printed circuit boards or ceramic materials, to support the transmission lines. Examples of substrate-based technologies include Microstrip, strip line, coplanar waveguide (CPW) and substrate integrated waveguide (SIW). These technologies have some advantages, such as low cost, easy fabrication and integration with other components. However, they also have some drawbacks, such as limited power handling capacity and dielectric loss that reduces the efficiency and performance of the power dividers. Moreover, some of these technologies, such as microstrip and strip line, have a high level of electromagnetic (EM) wave leakage that causes interference and crosstalk. This problem can be mitigated by using shielded structures, such as strip line and SIW, which confine the EM waves within the substrate [25], [26], [27], [28], [29], [30].

Another type of technology that can be used to design power dividers is conventional hollow waveguide, which is a full-metal structure that guides the EM wave through the air inside it. Hollow waveguide structures have some benefits, such as high efficiency and low loss, because the EM wave does not interact with any dielectric material. In addition, they can handle high power levels without damaging the device. However, they also have some limitations, such as fabrication challenges. Hollow waveguide structures are large and heavy, which makes them difficult to integrate with other components. Furthermore, they require high precision manufacturing process, which increases the cost of the overall wireless module. This is especially true for mmWave and high frequency applications, where the dimensions of the hollow waveguide are very small and any deviation in the manufacturing process can affect the performance of the device [31], [32], [33], [34], [35].

A new technology that has been proposed to solve the fabrication issues of the conventional waveguides is the gap waveguide technology [36]. This technology is based on creating a bandgap between two parallel plates, one made of PEC and the other is PMC. The bandgap is a frequency range where no EM wave can propagate between the plates. By designing a specific path for the EM wave on the PEC plate, such as a ridge or a groove, the EM wave can be guided along that path without any leakage. Therefore, there is no need for electrical contacts between different parts of the structure, which simplifies the fabrication process and reduces the cost of the device. Such semi open structures also allow integration of active components.

The PMC structure can be realized by using some periodic arrangements of metal pins that act as artificial magnetic materials [37]. These pins can be fabricated using different methods, such as die sink electrical discharge, molding, multilayer die pressing, electron beam melting, 3D printing and CNC milling. These methods are relatively cheap and easy to implement, which makes the gap waveguide technology more affordable and accessible. The gap waveguide technology has been applied to design various devices, such as power dividers [38], [39], [40], filters [41], [42], couplers [43], [44], planar antennas [45], [46], [47] and phase shifters [48], [49], which have shown promising results and performance.

In recent years, several power dividers have been reported based on the groove gap waveguide (GGW) technology. A H-plane power divider for array antenna design is reported in [38] with 33% impedance bandwidth and a slot array antenna is proposed based on the designed power divider. [46] proposed a ridge gap waveguide (RGW) power divider indicating 30% impedance bandwidth and then a 16-way planar power divider is proposed to feed some cavities with 4-raditing slots. The inverted microstrip gap waveguide (IMGW) technology has been used to form an unequal power divider which exhibits 18.5% impedance bandwidth; however, the efficiency of this power divider is limited due to the dielectric losses [50]. In [51], a power divider is proposed using combination of the RGW and E-plane GGW (E-GGW). The impedance bandwidth of this power divider is limited to 15%. A spatial power divider is reported in [52] in which a 4-way power divider is designed using irregular mirrors. The proposed power divider exhibits 29% bandwidth in Ka-band.

Moreover, different types of gap waveguide based power dividers have been reported including Magic-T [40], 3dB couplers [43], radial power divider [53] and six-port power divider [54] and Gysel power divider [55].

The reported power dividers do not have both wideband performance and compact size. Consequently, they are not the optimum choice for mmWave applications such as array antenna design. The reported antenna arrays have multi-layer structures, as the power divider usually feed a cavity to excite some radiating slots due to lack of the space.

This paper introduces a novel design of a power divider with compact size and wideband performance that uses a hybrid structure of E-plane groove gap waveguide and ridge gap waveguide. The proposed structure offers several advantages which can be summarized as follows:

- Compact size
- Low-loss and high efficiency
- Simple and single layer structure
- Wideband performance

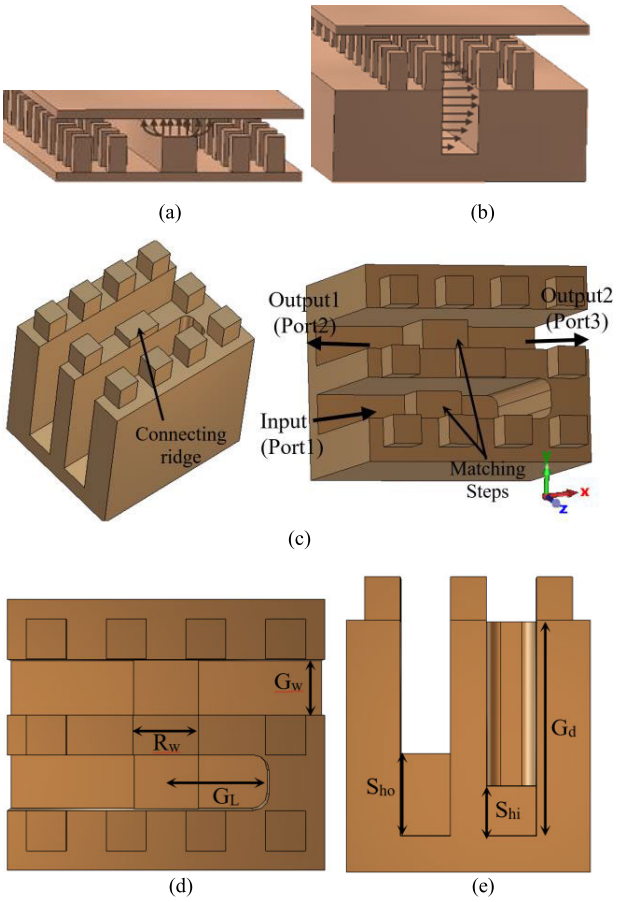

FIGURE 1. Geometries of the (a) ridge gap waveguide and (b) E-plane groove gap waveguide, and (c) perspective, (d) top and (e) side views of the proposed power divider.

- Good amplitude and phase balance of the outputs
- Convenient construction of multiple-output power divider

II. DESIGN OF THE PROPOSED POWER DIVIDER

In this section, the design of the proposed power divider is presented. The power divider is based on a combination of E-GGW and RGW. Fig. 1 illustrates the geometry of the E-GGW and RGW as well as the power divider. The power divider comprises two adjacent E-GGW that are coupled by a short RGW section. Therefore, the input and output ports of the power divider, which are E-GGW, are the same. The first step in the design process is to optimize the pin dimensions of the gap waveguide structure to ensure acceptable isolation with only one pin row, as the input and outputs are closely spaced and their coupling should be reduced in order to decrease the output amplitude imbalance. The CST Microwave Studio is employed to simulate and optimize the band gap of the periodic pins and Fig. 2(a) provides the optimized parameters and the simulated dispersion diagram. The optimized band gap extends from 35 GHz to 229 GHz, demonstrating a wideband performance. To evaluate the performance of the proposed pin structure, the isolation between two adjacent E-GGWs is simulated with only one pin row

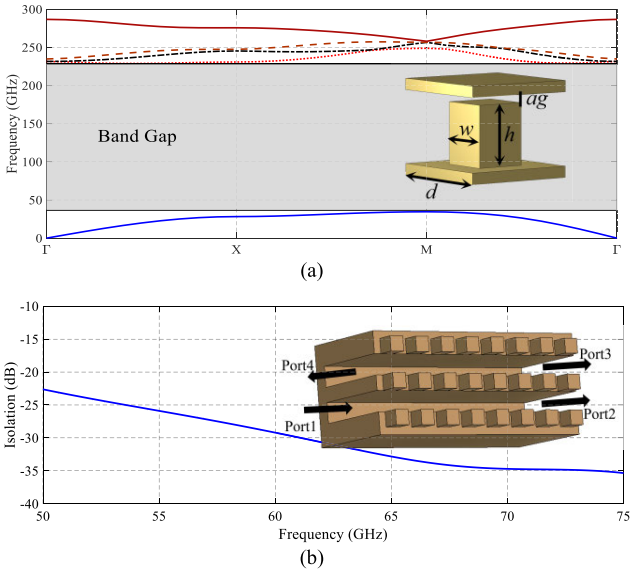

FIGURE 2. (a) dispersion diagram of the periodic pin structure. The pin dimensions are $w = 0.5$ mm, $h = 0.6$ mm, $d = 1$ mm and $ag = 0.01$ mm, (b) the isolation between two adjacent E-GGWs with one row pin.

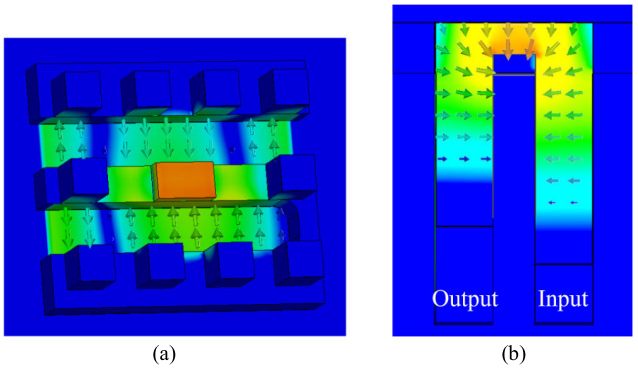

FIGURE 3. The simulated electric field distribution on the proposed power divider structure in (a) the perspective view and (b) the cross section.

between them. Fig. 2(b) depicts the structure which consists of two adjacent E-GGW with 4 ports. The structure is simulated by Port1 excitation and the isolation is calculated by Isolation $= |S_{31}| + |S_{41}|$ and the result is plotted in Fig. 2(b). As can be seen, one row pin structure provides isolation better than 23dB in the whole bandwidth which is satisfactory.

The geometry of the proposed power divider is illustrated in Fig. 1. It consists of two adjacent E-GGW along X-axis and a coupling RGW section along Y-axis. The impedance matching of the structure can be achieved by adjusting the height and width of the ridge and the length of the short-ended section of the input waveguide. As shown in Fig. 1(c), two steps are introduced inside the E-GGWs to enhance the matching and widen the impedance bandwidth of the structure. The width of the two steps is set to be equal to the ridge width while their heights are changing to tune the matching.

The simulated electric field distributions inside the structure are shown in Fig. 3(a) and (b), indicating that the outputs

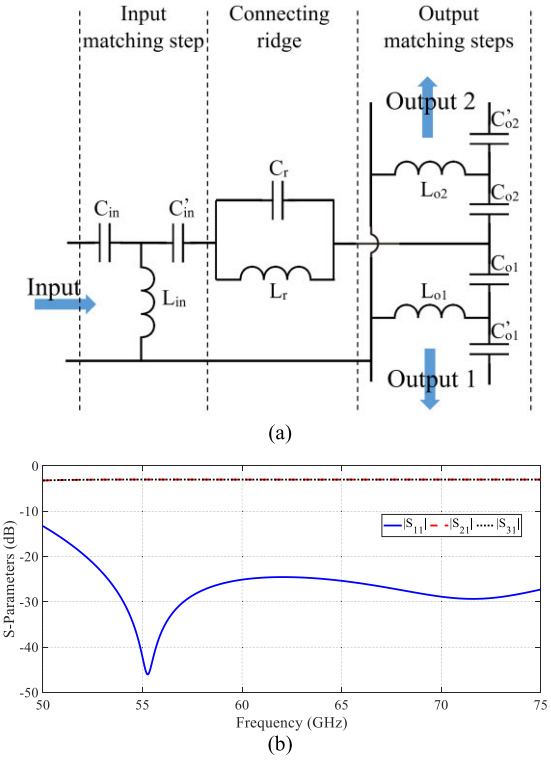

FIGURE 4. (a) A simplified equivalent circuit of the proposed power divider, (b) the S-parameters of the circuit model for $C_{in} = 0.07$ pf, $C'_{in} = 0.081$ pf, $L_{in} = 0.1$ nH, $C_r = 0.455$ pf, $L_r = 58$ nH, $C_{o1} = C_{o2} = 0.058$ pf, $C'_{o1} = C'_{o2} = 0.0495$ pf, $L_{o1} = L_{o2} = 143$ pH.

have the same amplitude and are in-phase. As shown in these figures, the EM energy couples from the input E-GGW to the coupling RGW and then, it couples in the output E-GGW and travels in both directions in equal amplitude and phase.

To investigate the bandwidth enhancement of the power divider, a simplified equivalent circuit of the power divider is proposed which is depicted in Fig. 4(a). According to [56], a metallic block placed at the narrow wall of a rectangular waveguide can be represented by an equivalent circuit of two series capacitors and a parallel inductor, as long as the block's edges are parallel to the electric field. This circuit model also can be applied to the matching steps in the E-GGW.

In this circuit model, the capacitors and inductor values depend on the height and width of the matching steps. By increasing the step height or width, the capacitance value is increased while the inductance value is decreased. In the proposed circuit model, which is depicted in Fig. 4(a), C_{in} and L_{in} are pertinent to the matching step in the input E-GGW. The second matching step in the output branch can be considered as two half metallic blocks which are connected together in the output ports and therefore, two circuit models are added to each output ports with values of C_{o1}, C'_{o1} and L_{o1} for the Output1 and C_{o2},C'_{o2} and L_{o2} for the Output2. As the output ports are symmetric, the height and width of two steps are the same and therefore, $C_{o1} = C_{o2}$, $C'_{o1} = C'_{o2}$ and $L_{o1} = L_{o2}$. If the output step is not symmetric, then the output circuit elements are not equal and therefore, an imbalance in the power divider outputs will be achieved. Moreover, the coupling ridge is modeled as a parallel LC resonant circuit (L_r and C_r) which couples the EM energy from the input waveguide section to the output sections. The S-parameters of the equivalent circuit is calculated using MATLAB which is shown in Fig. 4(b). As can be seen, the circuit has two resonances around 55 GHz and 72 GHz which leads to a wideband performance of the power divider.

To show the effects of circuit elements on the power divider performance, the structure is simulated for different values of these circuit parameter. Fig. 5(a) shows the effect of the ridge parameters on the reflection coefficient. In this case, the matching steps are removed and the structure consist of two E-GGWs and a coupling ridge and therefore, the power divider bandwidth is limited. As can be seen in Fig. 5(a), by elevating the ridge height, L_r is increased and consequently leading to a reduction in the resonant frequency. Also, by widening the connecting ridge width (r_w), C_r is increased which causes resonant frequency reduction.

By adding the matching steps, the bandwidth can be extended. To achieve the broadest possible bandwidth, the heights of the steps should be chosen such that one step has a resonant frequency at the lower frequency band, while the other one resonates at the upper band. Figs. 5(b) and (c) show the effects of the matching steps heights on the reflection coefficients. The input matching step height (S_{hi}) sets a resonance frequency in the upper band while the output matching step height (S_{ho}) sets a resonance in the lower frequencies. By adjusting these two resonances correctly, the bandwidth of the power divider section can be greatly improved.

If the output step is asymmetric, an imbalance in the output ports is achieved. Fig. 5(d) depicts the effect of asymmetric value (Δw) on the transmission coefficients. According to the results, around 2.5 dB power imbalance can be achieved by increasing Δw which is useful in the unequal power divider design.

The effect of the matching steps on the power divider outputs isolation is simulated and plotted in Fig. 5(e). As shown in the figure, the isolation is enhanced by introducing the matching steps. This matter can be concluded from the equivalent circuit as the output step is placed between output ports and it can enhance the outputs isolation due to its resonance behavior. The isolation is around 6dB in the whole bandwidth, as the power divider is lossless and it is very challenging to obtain a high level of isolation in lossless power dividers.

The design parameters of the power divider should be wisely optimized that has been carried out by utilizing the embedded Trust Region Framework optimizer of the CST Microwave Studio. Table 1 lists the optimized parameters and the S-parameters of the structure are plotted in Fig. 6. According to the simulated results, the proposed power divider exhibits 40% impedance bandwidth covering from 50 GHz to 75 GHz. The insertion loss of the structure is less than 0.15 dB almost in the entire bandwidth. Fig. 6(b) shows the

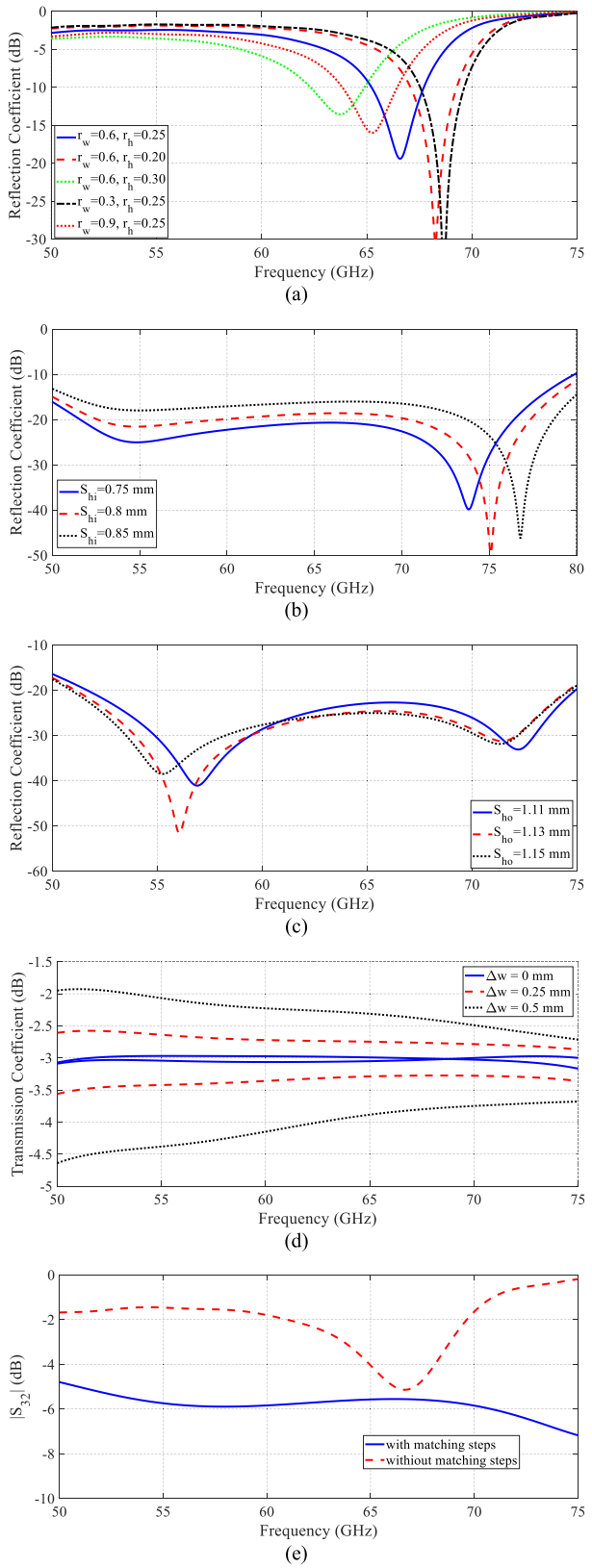

FIGURE 5. The effects of the design parameters on the power divider performance.

simulated phases of the outputs, which are in-phase throughout the bandwidth.

TABLE 1. Design parameters of the proposed power divider.

Symbol	Description	Value
G_w	Width of the E-GGW	0.7 mm
G_d	Depth of the E-GGW	3 mm
G_L	Length of the short-ended groove	1.7 mm
S_w	Width of the Ridge, input and output steps	0.82 mm
R_h	Height of the ridge	0.23 mm
S_{hi}	Height of the input step	0.7 mm
S_{ho}	Height of the output step	1.2 mm

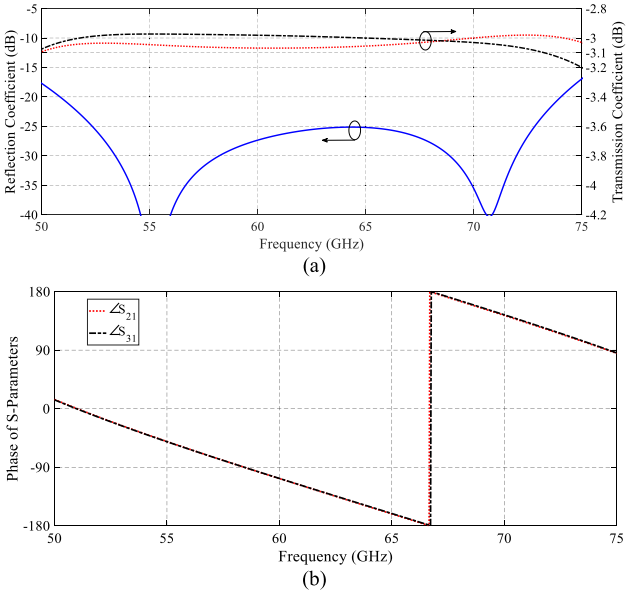

FIGURE 6. The simulated (a) amplitude and (b) phase of the proposed power divider S-parameters.

TABLE 2. Comparison of the reported 2-way power dividers.

Ref.	Tech.	Freq (GHz)	IBW*	IL*	size
[17]	HW*	11.3-12.6	11 %	0.2 dB	2.31λ × 1.72 λ
[38]	GGW	50-70	33 %	0.1 dB	1.2λ × 1.5 λ
[46]	RGW	50-68	30 %	0.15 dB	0.8λ × 1.1 λ
[50]	IMGW	36-44	20 %	0.17 dB	0.5λ × 0.75 λ
This work	RGW & EGGW	50-75	40 %	0.15 dB	0.58λ × 0.7 λ

* Hollow waveguide (HW), Impedance bandwidth (IBW) and Insertion loss (IL).

Table 2 compares the proposed power divider and the previously reported 2-way power dividers with different technology. It can be concluded that the proposed power divider has a compact size with wideband and high efficiency performance.

Moreover, as the input and output ports are parallel to each other, an advanced multi-way power divider can be formed by easily cascading the proposed power divider without any bends unlike the other power dividers topologies as shown in Fig. 7. This leads to a more compact structure. As instant, an 8-way linear power divider based on RGW is

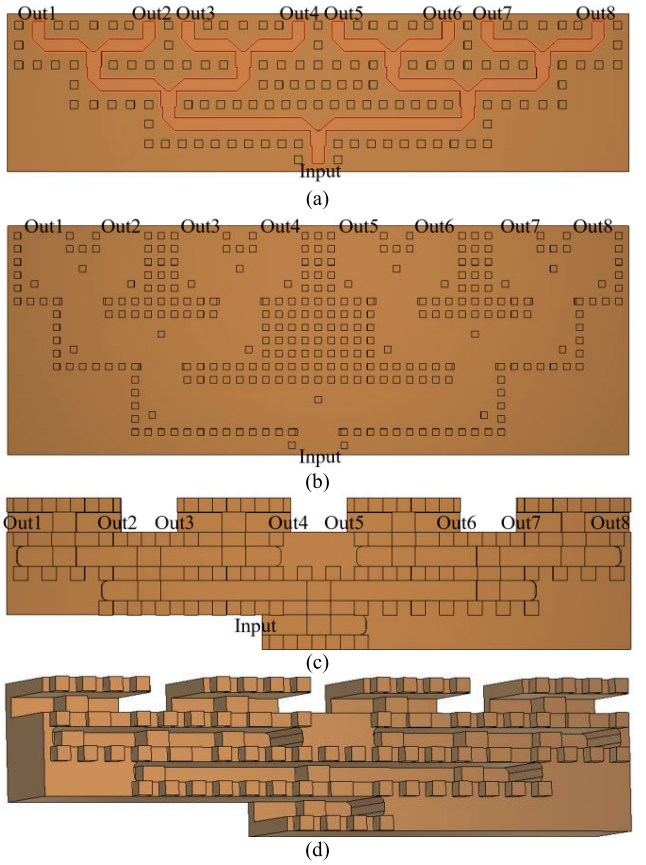

FIGURE 7. 8-way power dividers based on (a) RWG and (b) GGW and (c) the proposed 8-way power divider and (d) its perspective view.

presented in [57] which its size is about 4.7λ ×6.9 λ while an 8-way power divider based on the proposed method has about 1.1λ × 4.6λ. Fig. 7(a) and (b) show typical 8-way power dividers based on RGW and GGW, respectively to figure out the overall configuration of them.

To show the aforementioned advantages, an 8-way power divider is designed by cascading the proposed power divider as shown in Fig. 7(c), (d). The S-parameters of the designed power divider are plotted in Fig. 8. As shown, the impedance matching of the structure is acceptable in the whole bandwidth from 50 GHz to 75 GHz while the power imbalance is less than 0.7 dB. It is worth mentioning that the results are obtained just by cascading the 2-way power divider without any tuning or optimization which indicates the proposed power divider is robust and reliable.

III. BACK-TO-BACK 8-WAY POWER DIVIDER

To evaluate the performance of the proposed power divider, two 8-way power dividers are arranged in a back-to-back configuration as shown in Fig. 9. The output ports of the power divider are converted to a simple RGW using a transition as the RGW are commonly utilized in the power amplifying and other applications. In addition, to excite the structure by using a standard waveguide flange, a transition from WR15

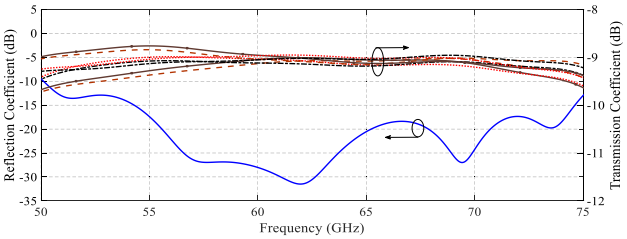

FIGURE 8. The simulated S-parameters of the proposed 8-way power divider.

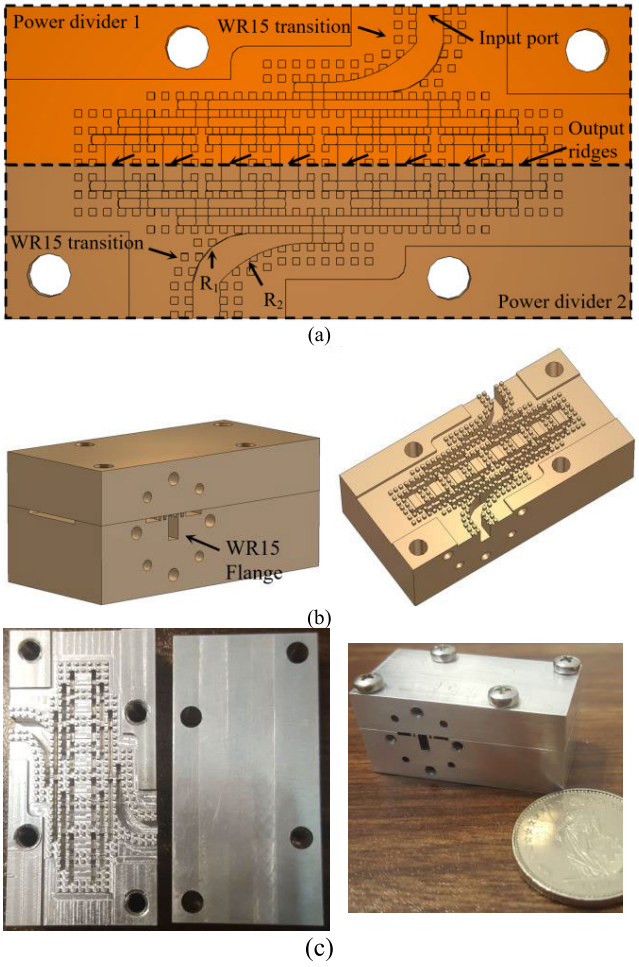

FIGURE 9. (a) top and (b) perspective views of the proposed back-to-back power divider, (c) photos of the fabricated device.

to E-GGW is designed and connected in the input and output ports as illustrated in Fig. 9.

This transition is a tapered bend which gradually matches the width and height of the E-GGW to the WR15 standard dimensions by rounding the both sides with R1 and R2 radiuses as shown in Fig. 9(a). The impedance matching is achieved by tuning the rounding radiuses that leads to optimized values of $R_1 = 3.96$ mm and $R_2 = 7.9$ mm. The reflection and transmission coefficients of the WR15 to EGGW transition are plotted in Fig. 10 which shows an excellent impedance matching of the transition.

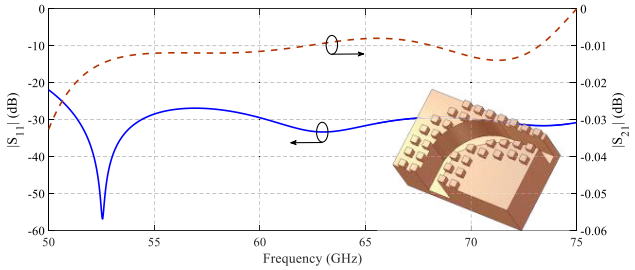

FIGURE 10. The reflection and transmission coefficients of the WR15 to E-GGW transition.

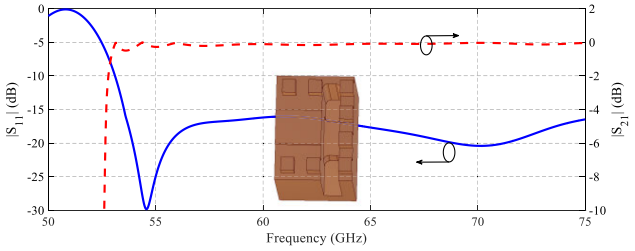

FIGURE 11. The reflection and transmission coefficients of the ridge to E-GGW transition.

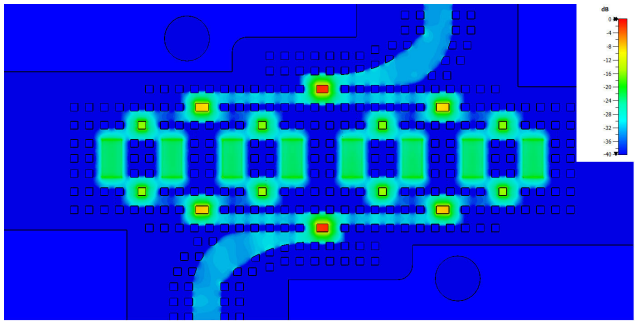

FIGURE 12. The electric field distribution on the back-to-back power divider structure.

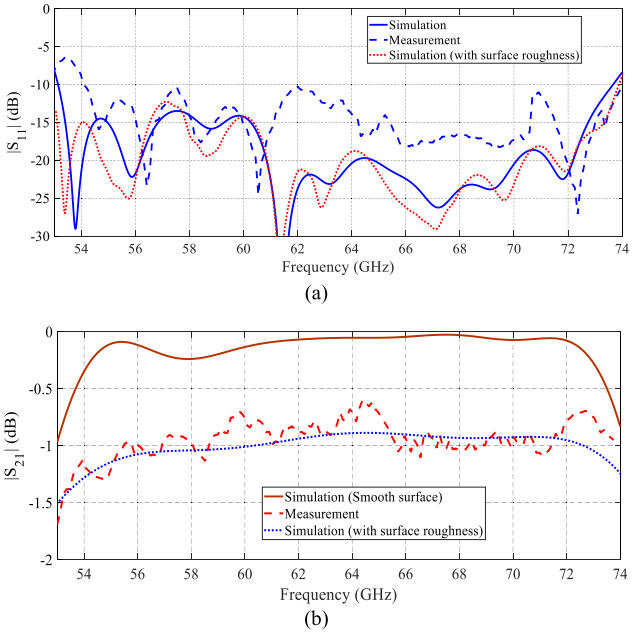

FIGURE 13. The simulated and measured reflection coefficients of the back-to-back power divider.

Furthermore, the S-parameter of the E-GGW to RGW (EG2R) transition is plotted in Fig. 11. The impedance bandwidth of the transition is 33% extending from 53 GHz to 74 GHz. The electric field distribution on the back-to-back structure is depicted in Fig. 12. As can be seen, all output branches have good amplitude balance. The simulated S-parameters of the back-to-back power divider are given in Fig. 13. The reflection coefficient of the structure is below -10 dB from 53 GHz to 74 GHz.

The impedance bandwidth of the back-to-back arrangement is narrower than the 8-way power divider as it is limited by the matching of the EG2R transition. The transmission coefficient is almost around -0.24 dB level and that shows the high efficiency of the power divider. The back-to-back power divider has been fabricated in Aluminum using CNC milling machine. The photos of the fabricated device are given in Fig. 9(c). The measured S-parameters of the power divider are plotted in Fig. 13. As shown, the measured S_{11} is similar to the simulated one. The S_{21} is around -1 dB which is due to the fabrication tolerance, surface roughness and milling. To demonstrate the effect of the fabrication tolerances, the back-to-back structure is simulated with 10 μm surface roughness which is plotted in Fig. 13. As can be seen, the simulation and measured S_{21} are in excellent agreement at this situation, however, the roughness has insignificant effect on the S_{11}.

IV. WIDEBAND LINEAR ARRAY ANTENNA DESIGN

In order to demonstrate an application of the proposed compact power divider, an 8-element linear array antenna is designed in which the radiating elements are E-plane horn antenna and the feeding network is the proposed power divider. The geometry of the E-plane horn antenna array is depicted in Fig. 14(a) that consists of a E-plane horn flare, a 90° bend and a transition from E-GGW to RGW. The complete array antenna including sub-array antenna, 8-way power divider and the WR15 to E-GGW transition is shown in Fig. 14(a). The overall dimensions of the antenna are $43\times19.6\times14.4$ mm^3. The designed antenna array has been fabricated using a conventional CNC milling method in Aluminum material. Figs. 14(b)-(d) show some photos of the array antenna and the measurement setup inside the anechoic chamber. The simulated with and without surface roughness and measurement reflection coefficient of the fabricated antenna array are plotted in Fig. 15. As can be seen, the S_{11} of the antenna is below -10 dB from 53 GHz to 74 GHz that indicates 33% impedance bandwidth of the antenna. The simulated and measured reflection coefficients show good agreement, except for a very minor frequency shift in the measurement which can be attributed to the fabrication tolerances and assembly of the metal blocks.

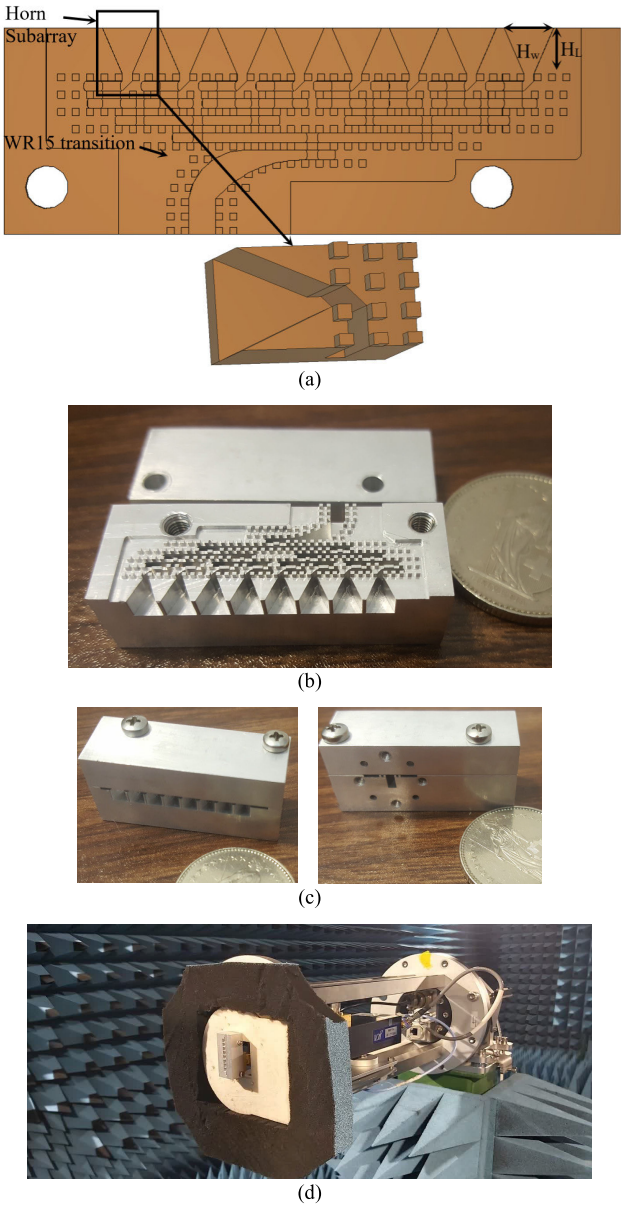

FIGURE 14. (a) top view of the proposed horn array antenna, photos of the fabricated (b) disassembled and (c) assembled horn array antenna and (d) the measurement setup inside the anechoic chamber.

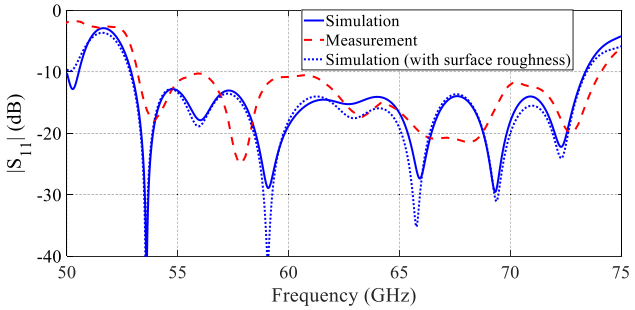

FIGURE 15. The simulated and measured reflection coefficient of the horn array antenna.

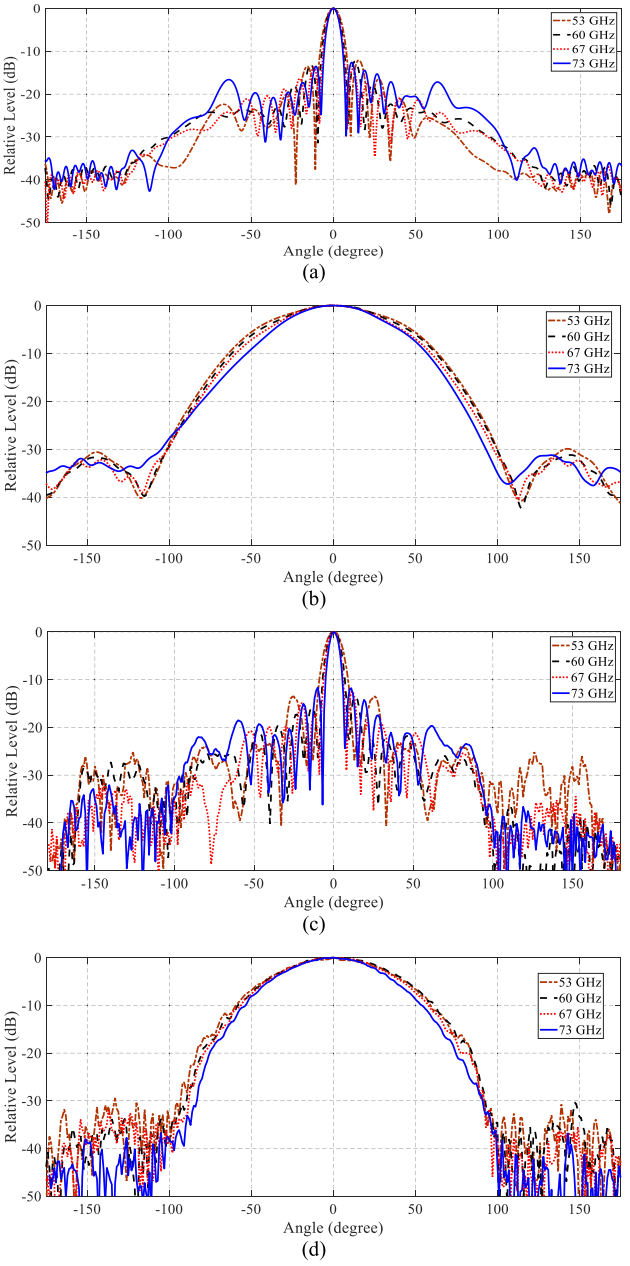

FIGURE 16. The simulated (a) E-plane and (b) H-plane normalized radiation patterns of the horn array antenna and the measured (c) E-plane and (d) H-plane ones.

TABLE 3. Comparison of the proposed array antenna with previously reported linear horn array antennas.

Ref.	Array size	Freq (GHz)	BW	Gain (dBi)	Efficiency
[57] 2018	1×4	27.5-38	32 %	14.2	78 %
[58] 2020	1×5	28.175	3 %	17.55	57 %
[59] 2022	1×20	73-80.2	9 %	17.5	80 %
[60] 2022	1×5	38.5-39.4	2.3 %	21	69 %
[61] 2023	1×4	45.5-55.4	20 %	18.6	85 %
This work	1×8	53-74	33 %	18.5	90 %

Fig. 16 shows the simulated and measured normalized radiation patterns in E- and H-planes at various frequencies. The radiation patterns are all satisfactory and show sidelobe levels which are quite close to theoretical limit of -13 dB level for an

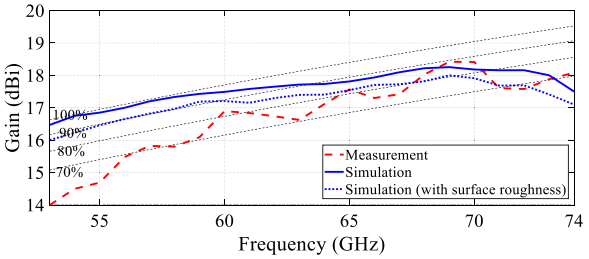

FIGURE 17. The simulated and measured gain of the horn array antenna and the efficiency lines.

equal amplitude and equal phase excitation of an array. Thus, the measured radiation patterns prove the proper amplitude distribution and phase balance of the proposed power divider over the entire bandwidth of the operating array.

Moreover, the antenna array gains are given in Fig. 17 for simulation with and without surface roughness and measurement. The roughness reduces the gain about 0.5 dBi. The maximum achieved gain is 18.5 dBi. The figure also includes the efficiency lines of the antenna. The results show that the measured antenna efficiency is mostly above 70%, with a peak of 90%, while the simulated efficiency reaches 97%.

The proposed array antenna is compared with similar linear horn array antennas in Table 3. As can be seen, the proposed array antenna has widest bandwidth while its efficiency is high.

V. CONCLUSION

This paper presents the design procedure of a new type of compact power divider based on gap waveguide technology. The proposed power divider is designed by combining E-plane groove and ridge gap waveguide structures. A wide impedance bandwidth of 40% is achieved for the proposed 2-way power divider while the insertion loss is less than 0.1 dB. Two 8-way power dividers are connected in a back-to-back arrangement to provide the possibility of the measurement test. In addition, a linear 8-elements horn array antenna is designed. The back-to-back structure and the array antenna were fabricated using a low-cost CNC milling technique. The measurement results prove the excellent performance of the proposed power divider. The results of this paper indicate that the proposed gap waveguide power divider is believed to be beneficial for mmWave application development.

REFERENCES

[1] T. Djerafi, A. Patrovsky, K. Wu, and S. O. Tatu, "Recombinant waveguide power divider," *IEEE Trans. Microw. Theory Techn.*, vol. 61, no. 11, pp. 3884–3891, Nov. 2013.

[2] S. Park, Y. Tsunemitsu, J. Hirokawa, and M. Ando, "Center feed single layer slotted waveguide array," *IEEE Trans. Antennas Propag.*, vol. 54, no. 5, pp. 1474–1480, May 2006.

[3] A. S. Sorokoa, A. O. Silin, V. I. Tkachenko, and I. S. Tsakanyan, "Simulation of multichannel waveguide power dividers (kharkov, Ukraine, September 15–17, 1998)," in *Proc. 3rd Int. Kharkov Symp. Phys. Eng. Millim. Submillimeter Waves. Symp.*, vol. 2, Kharkov, Ukraine, 1998, pp. 634–635.

[4] K. Kibaroglu, "28 GHz phased-array transceivers for 5G communications," Ph.D. dissertation, 2018. [online] Available: https://escholarship.org/uc/item/5rd2245w

[5] D. Deslandes, F. Boone, and K. Wu, "Universal single-layer waveguide power divider for slot array antenna applications," in *IEEE MTT-S Int. Microw. Symp. Dig.*, Jun. 2007, pp. 431–434.

[6] J.-C. S. Chieh, "A substrate-less microwave power-combining module utilizing ridge gap waveguide," *IEEE Microw. Wireless Compon. Lett.*, vol. 28, no. 11, pp. 972–974, Nov. 2018.

[7] M. P. DeLisio and R. A. York, "Quasi-optical and spatial power combining," *IEEE Trans. Microw. Theory Techn.*, vol. 50, no. 3, pp. 929–936, Mar. 2002.

[8] R. Maaskant, W. A. Shah, A. U. Zaman, M. Ivashina, and P.-S. Kildal, "Spatial power combining and splitting in gap waveguide technology," *IEEE Microw. Wireless Compon. Lett.*, vol. 26, no. 7, pp. 472–474, Jul. 2016.

[9] K. Song, Y. Fan, and Z. He, "Broadband radial waveguide spatial combiner," *IEEE Microw. Wireless Compon. Lett.*, vol. 18, no. 2, pp. 73–75, Feb. 2008.

[10] A. K. Pandey, "Broadband 32-way E-band inline power combiner for high-power MMIC amplifiers," in *Proc. 50th Eur. Microw. Conf. (EuMC)*, Utrecht, The Netherlands, Jan. 2021, pp. 864–867, doi: 10.23919/EuMC48046.2021.9337958.

[11] S. Farjana, E. Alfonso, P. Lundgren, V. Vassilev, P. Enoksson, and A. U. Zaman, "Multilayer dry film photoresist fabrication of a robust >100 GHz gap waveguide slot array antenna," *IEEE Access*, vol. 11, pp. 43630–43638, 2023, doi: 10.1109/ACCESS.2023.3271357.

[12] B. Xi, Y. Xiao, S. Tan, F. Yang, and Z. Chen, "2-bit wideband electronically controlled reconfigurable phased array with wide-angle beam-scanning capacity," *IEEE Trans. Antennas Propag.*, vol. 71, no. 5, pp. 4128–4137, May 2023, doi: 10.1109/TAP.2023.3256276.

[13] Q. You, Y. Lu, M. Huang, J. Xu, and J. Huang, "High-efficiency air-filled wideband ±45° dual-polarized slot array antenna," *IEEE Trans. Antennas Propag.*, vol. 71, no. 5, pp. 4582–4587, May 2023, doi: 10.1109/TAP.2023.3243256.

[14] Z. Cao, Y. Chen, and H. Meng, "A W-band two-dimensional monopulse sparse array antenna," *IEEE Trans. Antennas Propag.*, vol. 70, no. 10, pp. 9260–9269, Oct. 2022, doi: 10.1109/TAP.2022.3177417.

[15] W. Feng, X. Ni, R. Shen, H. Wang, Z. Qian, and Y. Shi, "High-gain 100 GHz antenna array based on mixed PCB and machining technique," *IEEE Trans. Antennas Propag.*, vol. 70, no. 8, pp. 7246–7251, Aug. 2022, doi: 10.1109/TAP.2022.3164208.

[16] Q. You, Y. Lu, Y. Wang, J. Xu, J. Huang, and W. Hong, "Hollow-waveguide tri-band shared-aperture full-corporate-feed continuous transverse stub antenna," *IEEE Trans. Antennas Propag.*, vol. 70, no. 8, pp. 6635–6645, Aug. 2022, doi: 10.1109/TAP.2022.3161265.

[17] J. L. Cano, A. Mediavilla, S. Dragas, and A. Tazon, "Novel square-waveguide dual-mode two-way reactive power divider," *IEEE Trans. Microw. Theory Techn.*, vol. 68, no. 3, pp. 980–986, Mar. 2020.

[18] D. Zarifi, A. Farahbakhsh, and A. U. Zaman, "A gap waveguide-based D-band slot array antenna with interdigital feed network," *IEEE Trans. Antennas Propag.*, early access, Sep. 5, 2023, doi: 10.1109/TAP.2023.3290080.

[19] A. M. Khan, M. M. Ahmed, U. Rafique, and S. Khan, "Design, analysis and fabrication of an inside-grooved slotted waveguide array antenna for HPM applications," *IEEE Access*, vol. 11, pp. 50116–50129, 2023, doi: 10.1109/ACCESS.2023.3277390.

[20] J.-K. Chuang, R.-Y. Fang, and C.-L. Wang, "Compact and broadband rectangular waveguide power divider/combiner using microstrip-fed antisymmetric tapered probe," *IEEE Trans. Compon., Packag., Manuf. Technol.*, vol. 4, no. 1, pp. 109–116, Jan. 2014, doi: 10.1109/TCPMT.2013.2264318.

[21] K. Song, Y. Fan, and Y. Zhang, "Eight-way substrate integrated waveguide power divider with low insertion loss," *IEEE Trans. Microw. Theory Techn.*, vol. 56, no. 6, pp. 1473–1477, Jun. 2008, doi: 10.1109/TMTT.2008.923897.

[22] M. M. Fahmi, J. A. Ruiz-Cruz, and R. R. Mansour, "Compact ridge waveguide Gysel combiners for high-power applications," *IEEE Trans. Microw. Theory Techn.*, vol. 67, no. 3, pp. 968–977, Mar. 2019, doi: 10.1109/TMTT.2018.2885521.

[23] L. Guo, J. Li, W. Fang, W. Huang, H. Shao, G. Deng, and S. Xie, "Design of rectangular waveguide to microstrip power dividers and their application as compact rectangular matching terminations," *IEEE Trans. Microw. Theory Techn.*, vol. 67, no. 12, pp. 4741–4750, Dec. 2019, doi: 10.1109/TMTT.2019.2944370.

[24] K. Song, F. Xia, Y. Zhou, S. Guo, and Y. Fan, "Microstrip/slotline-coupling substrate integrated waveguide power divider with high output isolation," *IEEE Microw. Wireless Compon. Lett.*, vol. 29, no. 2, pp. 95–97, Feb. 2019, doi: 10.1109/LMWC.2018.2888943.

[25] C.-W. Tang and J.-T. Chen, "A design of 3-dB wideband microstrip power divider with an ultra-wide isolated frequency band," *IEEE Trans. Microw. Theory Techn.*, vol. 64, no. 6, pp. 1806–1811, Jun. 2016, doi: 10.1109/TMTT.2016.2554552.

[26] A. Alhamed, G. Gültepe, and G. M. Rebeiz, "64-element 16–52-GHz transmit and receive phased arrays for multiband 5G-NR FR2 operation," *IEEE Trans. Microw. Theory Techn.*, vol. 71, no. 1, pp. 360–372, Jan. 2023, doi: 10.1109/TMTT.2022.3200415.

[27] I. Haroun, T.-Y. Lin, D.-C. Chang, and C. Plett, "A reduced-size, low-loss 57–86 GHz IPD-based power divider using loaded modified CPW transmission lines," in *Proc. Asia–Pacific Microw. Conf.*, Kaohsiung, Taiwan, Dec. 2012, pp. 1202–1204, doi: 10.1109/APMC.2012.6421869.

[28] R. Vincenti Gatti and R. Rossi, "Hermetic broadband 3-dB power divider/combiner in substrate-integrated waveguide (SIW) technology," *IEEE Trans. Microw. Theory Techn.*, vol. 66, no. 6, pp. 3048–3054, Jun. 2018, doi: 10.1109/TMTT.2018.2825347.

[29] M. Pasian, L. Silvestri, C. Rave, M. Bozzi, L. Perregrini, A. F. Jacob, and K. K. Samanta, "Substrate-integrated-waveguide e-plane 3-dB power-divider/combiner based on resistive layers," *IEEE Trans. Microw. Theory Techn.*, vol. 65, no. 5, pp. 1498–1510, May 2017, doi: 10.1109/TMTT.2016.2642938.

[30] C. A. Leal-Sevillano, J. A. Ruiz-Cruz, J. R. Montejo-Garai, and J. M. Rebollar, "Compact broadband couplers based on the waveguide magic-T junction," in *Proc. Eur. Microw. Conf.*, Nuremberg, Germany, Oct. 2013, pp. 151–154.

[31] U. Rosenberg and K. Beis, "Improved narrow-wall short slot coupler design exhibiting significant increased bandwidth and low cost production," in *Proc. 31st Eur. Microw. Conf.*, London, England, Oct. 2001, pp. 1–4.

[32] F. Alessandri, M. Giordano, M. Guglielmi, G. Martirano, and F. Vitulli, "A new multiple-tuned six-port riblet-type directional coupler in rectangular waveguide," *IEEE Trans. Microw. Theory Techn.*, vol. 51, no. 5, pp. 1441–1448, May 2003.

[33] J. Ding, Q. Wang, Y. Zhang, and C. Wang, "A novel five-port waveguide power divider," *IEEE Microw. Wireless Compon. Lett.*, vol. 24, no. 4, pp. 224–226, Apr. 2014.

[34] J. Ding, Q. Wang, Y. Zhang, L. Wu, and X. Sun, "High-efficiency millimetre-wave spatial power combining structure," *Electron. Lett.*, vol. 51, no. 5, pp. 397–399, Mar. 2015.

[35] P.-S. Kildal, E. Alfonso, A. Valero-Nogueira, and E. Rajo-Iglesias, "Local metamaterial-based waveguides in gaps between parallel metal plates," *IEEE Antennas Wireless Propag. Lett.*, vol. 8, pp. 84–87, 2009.

[36] P. -S. Kildal, A. U. Zaman, E. Rajo-Iglesias, E. Alfonso, and A. Valero-Nogueira, "Design and experimental verification of ridge gap waveguide in bed of nails for parallel-plate mode suppression," *IET Microw., Antennas Propag.*, vol. 5, no. 3, pp. 262–270, Feb. 2011.

[37] A. Farahbakhsh, D. Zarifi, and A. U. Zaman, "60-GHz groove gap waveguide based wideband *H*-plane power dividers and transitions: For use in high-gain slot array antenna," *IEEE Trans. Microw. Theory Techn.*, vol. 65, no. 11, pp. 4111–4121, Nov. 2017.

[38] A. Tamayo-Dominguez, J.-M. Fernandez-Gonzalez, and M. Sierra-Perez, "Groove gap waveguide in 3-D printed technology for low loss, weight, and cost distribution networks," *IEEE Trans. Microw. Theory Techn.*, vol. 65, no. 11, pp. 4138–4147, Nov. 2017.

[39] A. Farahbakhsh, "Ka-band coplanar magic-T based on gap waveguide technology," *IEEE Microw. Wireless Compon. Lett.*, vol. 30, no. 9, pp. 853–856, Sep. 2020.

[40] E. A. Alós, A. U. Zaman, and P.-S. Kildal, "Ka-band gap waveguide coupled-resonator filter for radio link diplexer application," *IEEE Trans. Compon., Packag., Manuf. Technol.*, vol. 3, no. 5, pp. 870–879, May 2013.

[41] Z.-H. Shi, F. Wei, L. Yang, and R. Gómez-García, "High-selectivity inverted microstrip gap waveguide bandpass filter using hybrid cavity and stub-loaded ring resonant modes," *IEEE Trans. Circuits Syst. II, Exp. Briefs*, vol. 71, no. 1, pp. 146–150, Jan. 2024.

[42] S. I. Shams and A. A. Kishk, "Design of 3-dB hybrid coupler based on RGW technology," *IEEE Trans. Microw. Theory Techn.*, vol. 65, no. 10, pp. 3849–3855, Oct. 2017.

[43] D. Zarifi, A. Farahbakhsh, and A. U. Zaman, "Design and fabrication of wideband millimeter-wave directional couplers with different coupling factors based on gap waveguide technology," *IEEE Access*, vol. 7, pp. 88822–88829, 2019.

[44] A. Vosoogh, M. S. Sorkherizi, A. U. Zaman, J. Yang, and A. A. Kishk, "An integrated Ka-band diplexer-antenna array module based on gap waveguide technology with simple mechanical assembly and no electrical contact requirements," *IEEE Trans. Microw. Theory Techn.*, vol. 66, no. 2, pp. 962–972, Feb. 2018.

[45] A. Farahbakhsh, D. Zarifi, and A. U. Zaman, "A mmWave wideband slot array antenna based on ridge gap waveguide with 30% bandwidth," *IEEE Trans. Antennas Propag.*, vol. 66, no. 2, pp. 1008–1013, Feb. 2018.

[46] A. U. Zaman and P.-S. Kildal, "Wide-band slot antenna arrays with single-layer corporate-feed network in ridge gap waveguide technology," *IEEE Trans. Antennas Propag.*, vol. 62, no. 6, pp. 2992–3001, Jun. 2014.

[47] H. Abdollahy, A. Farahbakhsh, and M. H. Ostovarzadeh, "Mechanical reconfigurable phase shifter based on gap waveguide technology," *AEU Int. J. Electron. Commun.*, vol. 132, Apr. 2021, Art. no. 153655, doi: 10.1016/j.aeue.2021.153655.

[48] E. Rajo-Iglesias, M. Ebrahimpouri, and O. Quevedo-Teruel, "Wideband phase shifter in groove gap waveguide technology implemented with glide-symmetric holey EBG," *IEEE Microw. Wireless Compon. Lett.*, vol. 28, no. 6, pp. 476–478, Jun. 2018.

[49] J. Liu, F. Yang, K. Fan, and C. Jin, "Unequal power divider based on inverted microstrip gap waveguide and its application for low sidelobe slot array antenna at 39 GHz," *IEEE Trans. Antennas Propag.*, vol. 69, no. 12, pp. 8415–8425, Dec. 2021.

[50] M. Ferrando-Rocher, A. Valero-Nogueira, and J. I. Herranz-Herruzo, "New feeding network topologies for high-gain single-layer slot array antennas using gap waveguide concept," in *Proc. 11th Eur. Conf. Antennas Propag. (EUCAP)*, Paris, France, 2017, pp. 1654–1657, doi: 10.23919/EuCAP.2017.7928169.

[51] M. Wang, Z. Wu, X. Liao, F. Li, Y. Pu, J. Wang, and Y. Luo, "Analysis and design of high-efficient high-power spatial power divider," *IEEE Trans. Antennas Propag.*, vol. 71, no. 7, pp. 6006–6013, Jul. 2023.

[52] B. Zhang, Y. Zhang, Z. Dang, H. Zhu, Y. Chen, and Z. Duan, "A compact and high-efficiency 220-GHz power amplifier module based on TE11-mode radial power combiner," *IEEE Trans. Microw. Theory Techn.*, vol. 72, no. 5, pp. 3118–3129, May 2024.

[53] D. Zarifi, A. Farahbakhsh, and A. U. Zaman, "A millimeter-wave six-port junction based on ridge gap waveguide," *IEEE Access*, vol. 11, pp. 68699–68705, 2023.

[54] A. K. Nobandegani and S. E. Hosseini, "Gysel power divider realized by ridge gap waveguide technology," *IEEE Access*, vol. 9, pp. 72103–72110, 2021.

[55] N. Marcuvitz, *Waveguide Handbook*. New York, NY, USA: McGraw-Hill, 1951.

[56] J. Benavides-Vazquez, J.-L. Vazquez-Roy, and E. Rajo-Iglesias, "On the use of ridge gap waveguide technology for the design of transverse stub resonant antenna arrays," *Sensors*, vol. 21, no. 19, p. 6590, Oct. 2021, doi: 10.3390/s21196590.

[57] N. Ashraf, A.-R. Sebak, and A. A. Kishk, "End-launch horn antenna array for Ka-band 5G applications," in *Proc. 18th Int. Symp. Antenna Technol. Appl. Electromagn. (ANTEM)*, Waterloo, ON, Canada, Aug. 2018, pp. 1–2.

[58] M. Ng Mou Kehn, C.-K. Hsieh, and E. Rajo-Iglesias, "Array of horns fed by a transverse slotted groove gap waveguide at 28 GHz," *Sensors*, vol. 20, no. 18, p. 5311, Sep. 2020.

[59] K. Lomakin, S. Alhasson, and G. Gold, "Additively manufactured amplitude tapered slotted waveguide array antenna with horn aperture for 77 GHz," *IEEE Access*, vol. 10, pp. 44271–44277, 2022.

[60] N. Castro, F. Pizarro, and E. Rajo-Iglesias, "High gain low profile horn array with circular polarization using a 3D printed anisotropic dielectric composite material at 38 GHz," *Sci. Rep.*, vol. 12, no. 1, p. 18944, Nov. 2022.

[61] M. S. H. S. El-Din, S. I. Shams, A. M. M. A. Allam, A. Gaafar, H. M. Elhennawy, and M. F. A. Sree, "Design of an E-sectoral horn based on PRGW technology for 5G applications," *Int. J. Microw. Wireless Technol.*, vol. 15, no. 6, pp. 1082–1090, Jul. 2023.

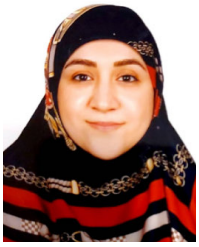

AREFEH KALANTARI KHANDANI was born in Kerman, Iran, in 1993. She received the B.Sc. degree in electrical engineering from the Azad University of Kerman, Kerman, in 2015, and the M.Sc. degree in electrical engineering from the Graduate University of Technology, Kerman, in 2023. Her current research interests include gap waveguide technology, antenna design, and microwave components.

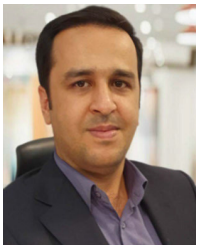

ALI FARAHBAKHSH was born in Kerman, Iran, in 1984. He received the Ph.D. degree in electrical engineering from Iran University of Science and Technology, Tehran, Iran, in 2016. He is currently an Associate Professor with the Department of Electrical and Computer Engineering, Graduate University of Advanced Technology, Kerman. Currently, he is a Guest Associate Professor with Gdansk University of Technology, Gdańsk, Poland, hosted by Prof. Michal Mrozowski. His research interests include microwave and antenna engineering, including gap waveguide technology, millimeter-wave high-gain array antenna, microwave devices, electromagnetic waves propagation and scattering, inverse problems in electromagnetic, and anechoic chamber design.

DAVOOD ZARIFI was born in Kashan, Iran, in 1987. He received the B.S. degree in electrical engineering from the University of Kashan, Kashan, in 2009, and the M.S. and Ph.D. degrees in electrical engineering from Iran University of Science and Technology (IUST), Tehran, Iran, in 2011 and 2015, respectively. He is currently an Associate Professor with the School of Electrical and Computer Engineering, University of Kashan. He is also a Guest Associate Professor with Gdansk University of Technology, Gdańsk, Poland, hosted by Prof. Michal Mrozowski. His research interests include the applications of metamaterials, microwave passive components, slot array antennas, and gap waveguide technology.

ASHRAF UZ ZAMAN (Senior Member, IEEE) was born in Chittagong, Bangladesh. He received the B.Sc. degree in electrical and electronics engineering from Chittagong University of Engineering and Technology, Chittagong, in 2001, and the M.Sc. and Ph.D. degrees from the Chalmers University of Technology, Gothenburg, Sweden, in 2007 and 2013, respectively. He is currently an Associate Professor with the Communication and Antenna Systems Division, Chalmers University of Technology. His current research interests include high-gain millimeterwave planar antennas, gap waveguide technology, frequency-selective surfaces, microwave passive components, RF packaging techniques, and low-loss integration of MMICs with the antennas.